Available online at www.sciencedirect.com
ScienceDirect
Ceramics International 38S (2012) S87–S90
CERAMICS INTERNATIONAL
www.elsevier.com/locate/ceramint

Solution-based fabrication and electrical properties of $CaBi_4Ti_4O_{15}$ thin films

Chien-Min Cheng [a,*], Kai-Huang Chen [b], Jen-Hwan Tsai [c], Chia-Lin Wu [d]

[a] Department of Electronic Engineering, Southern Taiwan University, Tainan, Taiwan, ROC
[b] Department of Electronics Engineering and Computer Science, Tung-Fang Design University, Kaohsiung, Taiwan, ROC
[c] Department of Mathematics and Physics, Chinese Air Force Academy, Kangshan, Taiwan, ROC
[d] Graduate School of Engineering Science and Technology, National Yunlin University of Science and Technology, Yunlin, Taiwan, ROC

Available online 30 April 2011

Abstract

Ferroelectric $CaBi_4Ti_4O_{15}$ (CBT) thin films were prepared by spin coating technology using solution-based fabrication. The as-deposited CBT thin films were crystallized below 600 °C and the layered perovskite were crystallized at 700 °C using CFA processing in air. The enhancement of ferroelectric properties in CBT thin films for MFIS structures were investigated and discussed. Compared the $Bi_4Ti_3O_{12}$ (BIT), the CBT showed the better physical and electrical characteristics. The 700 °C annealed CBT thin films on SiO_2/Si substrate showed random orientation and exhibited large memory window curves. The maximum capacitance, memory window and leakage current density were about 250 pF, 2 V, and 10^{-5} A/cm^2, respectively.

Keywords: Sol–gel process; C. Ferroelectric properties; D. Pervoskite; E. Capacitors

1. Introduction

The bismuth layer structured ferroelectrics (BLSFs) were excellent candidate materials for application in ferroelectric random access memories (FeRAMs) device such as in memory cards and portable electronic devices utilizing the low electric consumption, nonvolatility, high speed readout. Several functional ceramics of perovskite structures, such as lead zirconate, lead zinc niobate, barium titanate, and bismuth titanate were successfully synthesized and fabricated. They have low coercive fields, high remanent polarizations (P_r), fatigue-free, and low processing temperatures [1–5].

The bismuth titanate system based materials were an important role for FeRAMs applications. The bismuth titanate materials were given in a general formula of bismuth layer structure ferroelectric, $(Bi_2O_2)^{2+}(A_{n-1}B_nO_{3n+1})^{2-}$ (A = Bi, B = Ti). The high leakage current, high dielectric loss and domain pinning of bismuth titanate system based materials were caused by defects, bismuth vacancies and oxygen vacancies. These defects and oxygen vacancies were attributed from the volatilization of Bi_2O_3 of bismuth contents at elevated temperature [1–5].

Recently, the CBT material, with the nominal composition of $CaBi_4Ti_4O_{15}$, was a compound belonging to the bismuth layer family. The Curie temperature of CBT material around 790 °C was found by pervious study. In addition, it was expected to special application in high temperature [6,7].

Among various deposition methods such as, pulsed laser deposition, metalorganic chemical vapor deposition, rf magnetron sputtering, and sol–gel technology were used to fabricate the functional thin film. The advantages of polymeric precursor were the high stoichiometry control, the low temperature process and low cost method [1–7].

The leakage current density and the memory window of CBT thin films measured using the metal-ferroelectric-insulator-semiconductor (MFIS) structure were not developed and investigated before. The subject of this work was to study the possible application of CBT thin films deposited onto SiO_2/Si substrate using the solution-based fabrication. The physical and electrical characteristics of CBT thin films were deposited in the MFIS structures in this study. The leakage current

* Corresponding author. Tel.: +886 6 2533131x3143; fax: +886 6 2266739.
E-mail address: ccmin@mail.stut.edu.tw (C.-M. Cheng).

0272-8842/$36.00.
doi:10.1016/j.ceramint.2011.04.056

density, capacitance, and the memory window of CBT thin films were characterized.

2. Experimental

In this study, the ferroelectric CBT thin films were fabricated on SiO_2/Si(1 0 0) substrates by solution-based fabrication technology. The calcium nitrate [$Ca(NO_3)_2$-$4H_2O$], bismuth nitrate [$Bi(NO_3)_3$-$5H_2O$], and titanium isopropoxide [$Ti(OCH(CH_3)_2)_4$] were used as starting materials for calcium, bismuth, and titanium elements. Bismuth nitrate was dissolved in ethylene glycol solvent were stirred for 50 min at 120 °C. After the solution cooling to 80 °C for reflux 20 min, the CH_3COOH was added to the solution were stirred for 50 min at 120 °C. Then, titanium isopropoxide was added to solution were stirred 1 h at 120 °C. The calcium nitrate was added to solution and stirred 50 min at 120 °C. The ratio of Ca:Bi:Ti:CH_3COOH is 1:4:4:9 in this solution. The CBT sol–gel solution, with the nominal composition of $CaBi_4Ti_4O_{15}$, was fabricated from the above process. The solutions were spin coated on SiO_2/Si substrate at 3000 rpm for 20 s. The as-deposited thin films were dried at 150 °C for 1 min using hot plate. Subsequently, the as-deposited thin films were heat treatment at 350 °C for 3 min and then annealing at 600–700 °C for 1 h in air using a conventional furnace annealing (CFA). To increase the thickness of thin film to about 300 nm, spin-coating, drying, hot treatment and annealing were repeated 3 times.

The MFIS structures were made on a polished p-Si wafer of nominal resistivity ∼1.0 Ω cm. The SiO_2 buffer layer for 100 nm thickness was grown by wet thermal oxidation of the silicon wafer at 1100 °C for MFIS devices. The crystal structures of the as-deposited CBT thin films were determined by X-ray diffraction (SIEMENS D5000) analysis obtained using a Cu Kα radiation in the 2θ range of 20–60°. The surface microstructure was observed using scanning electron microscopy (SEM) morphology. To complete the MFIS structures, an array of circular top and bottom contacts with an area of 0.00785 cm^2 was formed by depositing a 500 nm thick aluminum (Al) film using the thermal evaporation method. The capacitance and leakage current characteristics of CBT thin films were measured using a gain phase analyzer (HP 4194A) and a semiconductor parameter analyzer (HP 4156). All the capacitance results of the CBT thin film were measured at 100 kHz, with the initial dc bias at the top electrode scanned between −20 and 20 V.

3. Results and discussion

The XRD pattern was used to identify the change on crystalline structures of as-deposited CBT and BIT thin films. From the XRD pattern, the crystalline orientations of (1 1 7), (0 0 8) and (0 0 6) planes were apparently observed in Fig. 1. It was found that the as-deposited CBT thin films consisted of the preferred (0 0 8) and (1 1 9) orientation. The BIT and CBT thin films were well *c*-axis oriented, but CBT thin film was more *c*-axis oriented than BIT. For the polycrystalline CBT thin films,

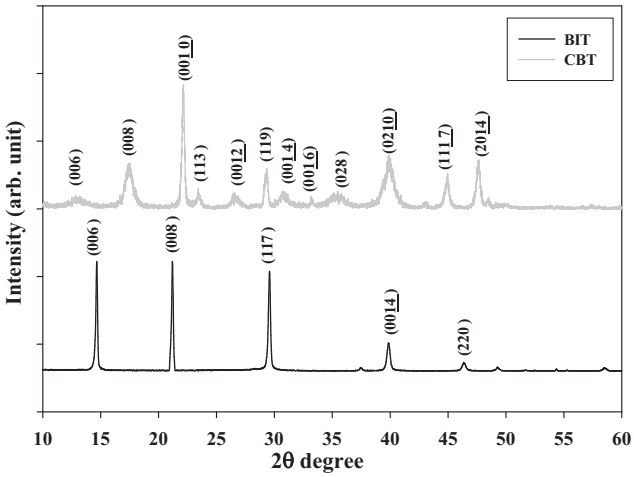

Fig. 1. The XRD patterns of as-deposited BIT and CBT thin films.

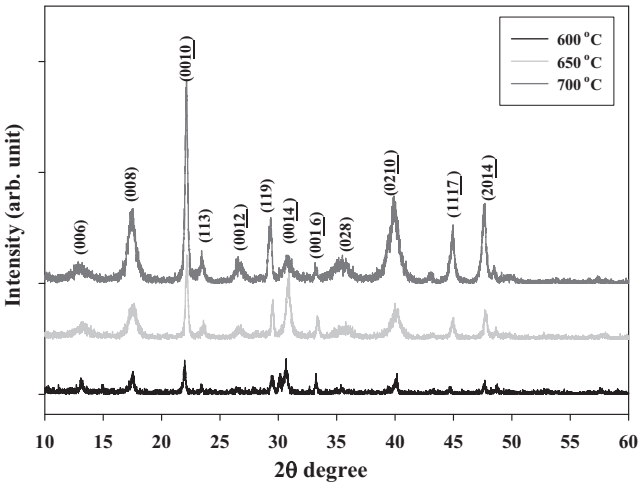

Fig. 2. The XRD patterns of as-deposited CBT thin films for different annealing temperature.

the (0 0 8) peak was the strongest peak in both of thin films. The change in the (0 0 8) and (0 0 6) orientation was observed except for the degree of the (1 1 9) orientation of CBT thin films. The XRD patterns of the as-deposited CBT thin films under different annealing temperature were observed in Fig. 2. These results indicated that the crystalline characteristics of annealed-CBT thin films were better than those of as-deposited CBT thin films. The crystallization characteristics of as-deposited CBT thin films were influenced by annealing temperatures process. The electrical and ferroelectric characteristics of as-deposited CBT thin films for 350 °C hot treatment under different annealing temperature will be further developed.

In Fig. 3, circular-like grains of as-deposited CBT thin films with 25 nm width were observed by SEM. From the cross-sectional morphology, the thicknesses of the CBT thin film were about 150 nm. In addition, the surface morphology and micro-structure of as-deposited CBT thin films under the CFA process were shown in Fig. 4. We found that the grain size of as-deposited CBT thin films increased while the annealing

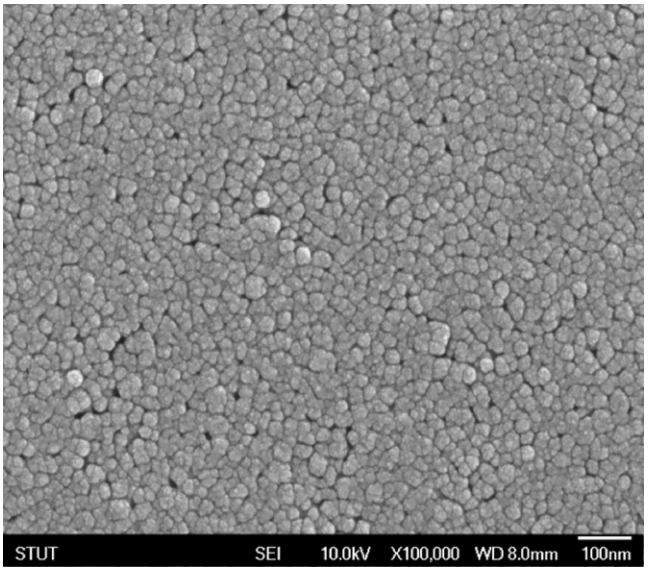

Fig. 3. The surface observation of the as-deposited CBT thin films.

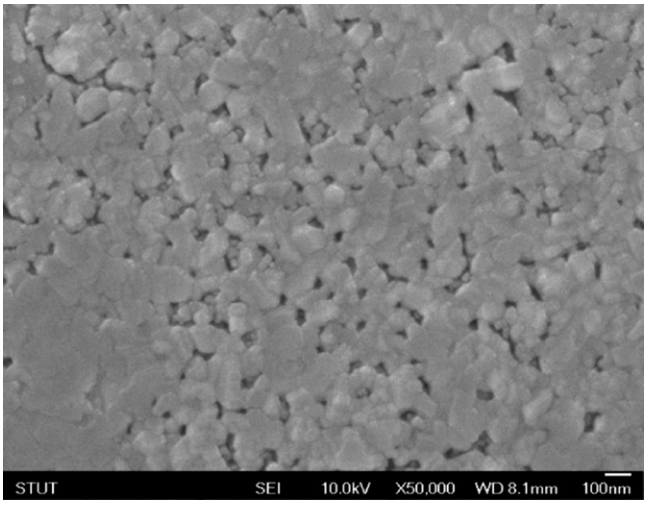

Fig. 4. The surface observation of the as-deposited CBT thin films annealed at 700 °C.

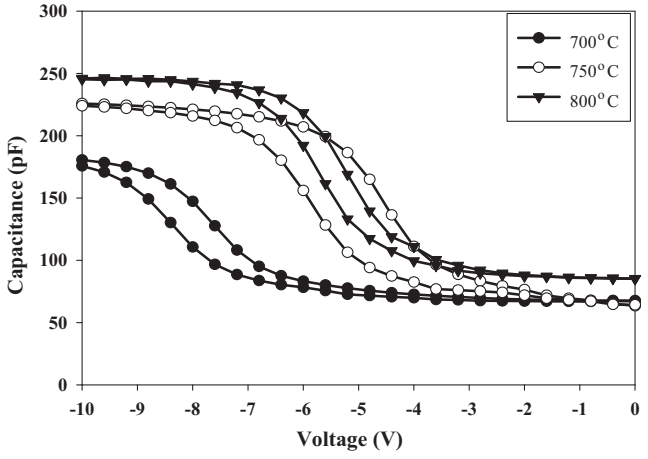

Fig. 5. The *C–V* curves for as-deposited CBT thin films annealed at 700–800 °C.

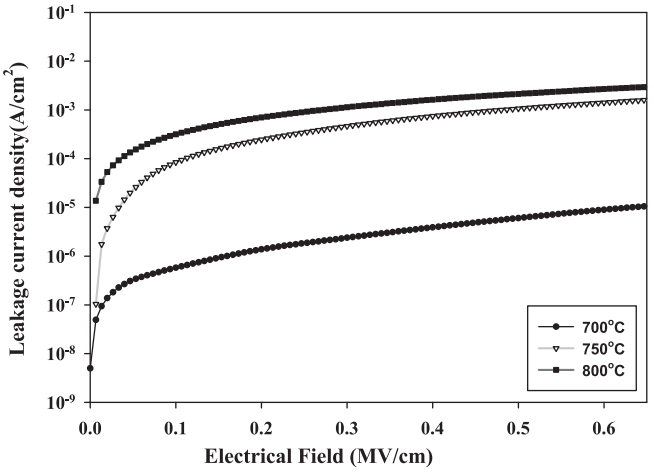

Fig. 6. Leakage current density in dependence of voltage for as-deposited CBT thin films annealed at 700–800 °C.

temperature increased to 700 °C. The surface of the grains size increased and the porosities of the as-deposited CBT thin film were followed the annealed temperature increased.

Fig. 5 shows the capacitance–voltage (*C–V*) curves of the as-deposited and annealed CBT thin films in air atmosphere for 1 h by CFA process. The applied voltages, which were first changed from −20 to 20 V and then returned to −20 V, were used to measure the capacitance voltage characteristics (*C–V*) of the MFIS structures. After CFA process, memory window of MFIS structure increased from 1 V to 2.2 V, and threshold voltage decreased from −5 V to −2 V. We revealed that the large memory window and high capacitance of the CBT thin film contributed the large grain size. These results demonstrated that low threshold voltage of the annealed-CBT thin films for MFIS structure caused by oxygen vacancy decreased.

Fig. 6 shows the leakage current density versus applied voltage curves of as-deposited and annealed CBT thin films on the MFIS structure. We found that the leakage current density of the annealed CBT thin films were larger than those of as-deposited CBT thin films. At an electric field of 0.5 MV/cm, the leakage current density of the 700 °C annealed CBT thin films

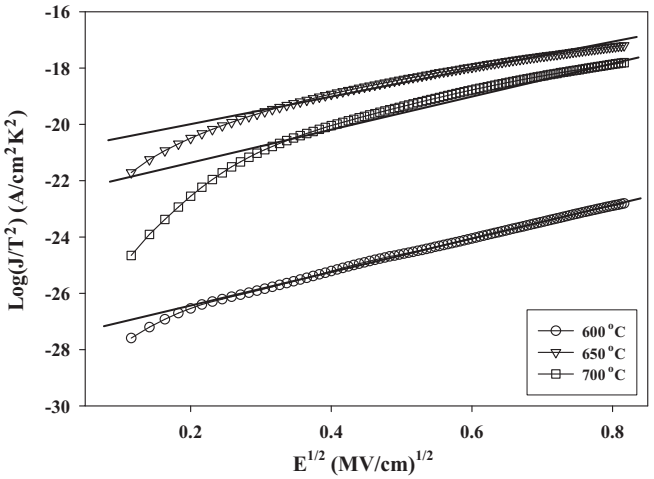

Fig. 7. The J/T^2 versus $E^{1/2}$ curves of as-deposited CBT thin films.

was increased from the 1×10^{-6} A/cm^2 to 1×10^{-4} A/cm^2 for high annealing temperature. This result indicated that the appropriate annealing temperature was effective method in lowering leakage current density of as-deposited CBT thin film.

To analyze that the phenomenon of oxygen vacancies and defect decreased of the annealed CBT thin films under the high annealing temperatures, the Schottky emission transport and Poole–Frenkel transport models were used to discuss the mechanism [8,9]. Fig. 7 showed the ln J/T^2 versus $E^{1/2}$ curves of annealed CBT thin films under 700 °C CFA annealing process. The annealed CBT thin films exhibited the Schottky emission transport mechanism and the as-deposited CBT thin films showed the Poole–Frenkel transport mechanism. These experimental results suggested that oxygen vacancies of the annealed CBT thin films decreased under the 700 °C CFA process in air atmosphere. However, the high leakage current density of the 800 °C annealed CBT thin films were attributed to the large grain boundary.

4. Conclusions

In conclusion, the as-deposited CBT thin films were prepared by solution-based fabrication technology. We investigated the CFA process treatment on electrical and physical properties of as-deposited CBT thin films for MFM structure at the annealing temperatures 700–800 °C. The as-deposited CBT thin film exhibited low leakage current characteristics. The leakage current density was 1×10^{-7} A/cm^2 as an applied electric field of 0.5 MV/cm applied. The memory window of MFIS structure increased from 1 V to 2.2 V, and threshold voltage decreased from −5 V to −2 V. The low threshold voltage of the annealed-CBT thin films for MFIS structure was caused by oxygen vacancy decreased. Finally, we found that electrical and physical characteristics of as-deposited CBT thin films improved by CFA treatment process from the XRD, SEM, *C–V* and *J–E* results.

References

[1] S.R. Shannigrahi, H.M. Jang, Fatigue-free lead zirconate titanate-based capacitors for nonvolatile memories, Applied Physics Letter 79 (2001) 1051–1053.

[2] K.H. Chen, Y.C. Chen, C.F. Yang, T.C. Chang, Fabrication and characteristics of $Ba(Zr_{0.1}Ti_{0.9})O_3$ thin films on glass substrate, Journal of Physics and Chemistry of Solids 69 (2008) 461–464.

[3] C.F. Yang, K.H. Chen, Y.C. Chen, T.C. Chang, Fabrication of one-transistor-capacitor structure of nonvolatile TFT ferroelectric RAM devices using $Ba(Zr_{0.1}Ti_{0.9})O_3$ gated oxide film, IEEE Ultrasonic Ferroelectric and Frequency Control 54 (2007) 1726–1730.

[4] C.F. Yang, K.H. Chen, Y.C. Chen, T.C. Chang, Physical and electrical characteristics of $Ba(Zr_{0.1}Ti_{0.9})O_3$ thin films under oxygen plasma treatment for applications in non-volatile memory devices, Applied Physics A 90 (2008) 329–331.

[5] K.H. Chen, Y.C. Chen, Z.S. Chen, C.F. Yang, T.C. Chang, Temperature and frequency dependence of the ferroelectric characteristics of $BaTiO_3$ thin films for nonvolatile memory applications, Applied Physics A 89 (2007) 533–536.

[6] K. Kazumi, S. Kazuyuki, N. Kaori, M. Takeshi, Ferroelectric properties of alkoxy-derived $CaBi_4Ti_4O_{15}$ thin films on Pt-passivated Si, Applied Physics Letter 78 (2001) 1119–1121.

[7] A.Z. Simões, M.A. Ramírez, A.H.M. Gonzaleza, C.S. Riccardia, A. Riesa, E. Longoa, J.A. Varelaa, Control of retention and fatigue-free characteristics in $CaBi_4Ti_4O_{15}$ thin films prepared by chemical method, Journal of Solid State Chemistry 179 (2006) 2206–2211.

[8] T. Mihara, H. Watanabe, Electronic conduction characteristics of sol–gel ferroelectric $Pb(Zr_{0.4}Ti_{0.6})O_3$ thin-film capacitors. Part I, Japan Journal of Applied Physics 34 (1995) 5664–5673.

[9] Y.-B. Lin, J.Y.-m. Lee, The temperature dependence of the conduction current in $Ba0.5Sr0.5TiO_3$ thin-film capacitors for memory device applications, Journal Applied Physics 87 (2000) 1841–1843.